International Journal of Medical Microbiology 310 (2020) 151436

Contents lists available at ScienceDirect

International Journal of Medical Microbiology

journal homepage: www.elsevier.com/locate/ijmm

Transcriptional regulation of virulence factors Hla and phenol-soluble modulins α by AraC-type regulator Rbf in *Staphylococcus aureus*

Bo Fang, Banghui Liu, Baolin Sun*

Department of Oncology, The First Affiliated Hospital, Division of Life Sciences and Medicine, University of Science and Technology of China. Anhui, Hefei 230027, China

ARTICLE INFO

Keywords:
Staphylococcus aureus
Rbf
Hla
PSMα
Virulence control

ABSTRACT

Staphylococcus aureus is a gram-positive pathogenic bacterium and is capable of secreting numerous toxins interfering directly with the host to cause acute infections. Rbf, a transcriptional regulator of AraC/XylS family, has been reported to promote biofilm formation in polysaccharide intercellular adhesion (PIA) mediated manner to cause chronic infections. In this study, we revealed the new virulence-mediated role of Rbf that can negatively regulate the hemolytic activity. Furthermore, Rbf can specifically bind to the *hla* and *psmα* promoters to repress their expression, resulting in significantly decreased production of phenol-soluble modulins α (PSMα) and alpha-toxin. Accordingly, the *rbf* mutant strain exhibited the increased pathogenicity compared to the wild-type (WT) strain in a mouse subcutaneous abscess model, representing a type of acute infection by *S. aureus*. Collectively, our results provide a novel insight into the virulence regulation and acute infections mediated by Rbf in *S. aureus*.

1. Introduction

Staphylococcus aureus is a major human pathogen for leading causes of morbidity and mortality from community- and hospital-acquired infectious diseases. These infectious diseases range from minor skin lesion to life-threatening sepsis pneumonia and toxic shock (Archer and Climo, 2001; Lowy, 1998). The virulence feature of *S. aureus* as a pathogen is mainly due to the fact that *S. aureus* can produce a large arsenal of virulence factors, including toxins, proteases, and secreted exoproteins (Bunikowski et al., 2000; Dinges et al., 2000; Foster, 2005). Among these, the production of toxins is necessary for acute infections by *S. aureus*. For instance, alpha-toxin and PSMα, as membrane-damaging toxins, play a critical role in the frequent types of acute *S. aureus* infections, including skin and blood infections (Oliveira et al., 2018; Foster, 2005; Nakagawa et al., 2017; Otto, 2014). The production of virulence factors is under control of diverse regulatory factors, of note, two-component systems and SarA family proteins (Arvidson and Tegmark, 2001; Bronesky et al., 2016; Cheung et al., 2004).

Rbf was originally identified as a transcriptional regulator, and contained a consensus region signature of AraC/XylS family, which can modulate the glucose- and NaCl-induced biofilm formation in *S. aureus* (Gallegos et al., 1997; Lim et al., 2004). Later, the mechanisms of this modulation revealed that Rbf can inhibit the transcriptional regulator IcaR, a negative regulator of *icaADBC*, then lead to increased production of polymeric N-acetylglucosamine (PNAG) to promote the biofilm formation (Cue et al., 2009). Recently, studies have demonstrated that Rbf can directly upregulate *sarX*, a member of *sarA* family, which then activates *icaADBC* by downregulating IcaR (Cheung et al., 2008; Cue et al., 2013). Biofilm formation is often involved in chronic infections and pronounced toxin production is characterized to be responsible for acute infections. These are the two main virulence traits that can affect the staphylococcal infections (Otto, 2014; Rupp et al., 1999a, b). Although Rbf has been recognized to play a major role in biofilm formation, its involvement in the regulation of acute infections has been unknown.

In the present study, we identified the novel role of Rbf in virulence control. We have found that the hemolytic activity was significantly increased in the*rbf* mutant strain compared to that in the WT strain. We further revealed that Rbf can directly bind *hla* and *psmα* promoters specifically to repress their expression. Moreover, the *rbf* mutant strain exhibited significantly enhanced pathogenicity in the mouse abscess infection model.

2. Materials and methods

2.1. Bacterial strains, plasmids, and growth conditions

The bacterial strains and plasmids used in this study are

* Corresponding author.
E-mail address: sunb@ustc.edu.cn (B. Sun).

https://doi.org/10.1016/j.ijmm.2020.151436
Received 24 December 2019; Received in revised form 25 May 2020; Accepted 14 June 2020

Table 1
Strains and plasmids used in this study.

Strain or plasmid	Description	Reference or source
Strains		
S. aureus		
NCTC8325 WT	NCTC8325 wild-type strain	NARSA[a]
RN4220	NCTC8325-4 r$^-$, initial recipient for modification of plasmids that are introduced into *S. aureus* from *E. coli*	NARSA
MW2 WT	CA-MRSA, SCCmec type IV	NARSA
NCTC8325 Δ*rbf*	NCTC8325 *rbf* mutant strain	(Ma et al., 2017)
NCTC8325 C-*rbf*	NCTC8325 *rbf* mutant strain harboring an introduced chromosomal copy of rbf for genetic complementation	This study
MW2 Δ*rbf*	MW2 *rbf* mutant strain	This study
MW2 C-*rbf*	MW2 *rbf* mutant strain harboring an introduced chromosomal copy of *rbf* for genetic complementation	This study
NCTC8325 WT pOS*hla*	NCTC8325 wild-type strain with pOS*hla*	This study
NCTC8325 Δ*rbf* pOS*hla*	NCTC8325 *rbf* mutant strain with pOS*hla*	This study
NCTC8325 WT pOS*psmα*	NCTC8325 wild-type strain with pOS*psmα*	This study
NCTC8325 Δ*rbf* pOS*psmα*	NCTC8325 *rbf* mutant strain with pOS*psmα*	This study
E.coli		
Trans5α	clone host strain	TransGen
BL21 (DE3)	expression strain	TransGen
Plasmids		
pBTs	shuttle vector, temperature sensitive, Ap^r Cm^r [b]	(Hu et al., 2015)
pBTs-up-*rbf*-down	pBTs derivative, for *rbf* chromosomal complementation, Ap^r Cm^r	This study
pLI50	shuttle cloning vector, Ap^r Cm^r	Addgene
pLI*rbf*	pLI50 derivative, harboring ORF of *rbf* and its promoter, Ampr Chlr	This study
pET28a (+)	expression vector with hexahistidine tag, Kan^r	This study
pOS1-*lacZ*	shuttle vector, containing promoter-less *lacZ* gene, Ap^r Cm^r	(Liu et al., 2011)
pOS*hla*	*hla-lacZ* fusion shuttle vector, a derivative of pOS1-*lacZ*	This study
pOS*psmα*	*psmα-lacZ* fusion shuttle vector, a derivative of pOS1-*lacZ*	This study

[a] NARSA, Network on Antimicrobial Resistance in *Staphylococcus aureus*.
[b] Kan^r, kanamycin-resistant; Ap^r, ampicillin-resistant; Cm^r, chloramphenicol-resistant.

summarized in Table 1. *Escherichia coli* strains were grown (220 rpm) in lysogeny broth (LB) medium or on lysogeny broth agar (LA) at 37°C. *Staphylococcus aureus* strains were grown (220 rpm) in tryptic soy broth (TSB) (Difco) or on tryptic soy agar plates (Difco) at 37°C. *S. aureus* strain RN4220 was used as a gateway strain prior to the propagation of plasmids into *S. aureus* NCTC8325 and MW2. When required, 150 μg/mL ampicillin sodium salt or 50 μg/mL kanamycin sulfate for *E. coli* or 15 μg/mL chloromycetin for *S. aureus* strains was added to the bacterial cultures.

2.2. DNA manipulation

*S. aureus*NCTC8325 and MW2 genomic DNA were prepared by a standard protocol for gram-positive bacteria (Cheng and Jiang, 2006). Plasmid DNA was extracted with a plasmid purification kit (Sangon Biotech) according to the manufacturer's instructions. Easy Taq DNA polymerase (TransGen) was used for PCR amplification to verify whether a correct sequence was cloned in. Primer STAR HS DNA polymerase (TaKaRa) was used for fragment PCR amplification to construct a plasmid. All plasmids from *E. coli* were transformed into *S. aureus* strain RN4220 for modification before transformed into the target *S. aureus* strains by electroporation, as described previously (Kraemer and Iandolo, 1990).

2.3. Expression and purification of Rbf

Expression and purification of the 2×FLAG-tagged Rbf were performed using the procedures as previously described (Ma et al., 2017). FLAG-taq, a fusion tag consisting of eight amino acids (AspTyrLysAspAspAspAspLys), was designed for labeled fusion proteins (Einhauer and Jungbauer, 2001). The fragment covering full-length Rbf open reading frame (ORF) and its corresponding promoter region was amplified with the E-*rbf*-F and E-*rbf*-R primers (Table 2), cloned into pLI50, and transformed into *S. aureus* RN4220. After grown in TSB at 37°C to an OD_{600} of 6.0, 100 g transformant cells were collected. Cell extracts were prepared as previously described (Cai et al., 2009; Takagi et al., 2005), then the extract suspension with our fusion protein was clarified by centrifugation (remove mainly body of lysed cells) and incubated for 2 h at 4°C with 1 mL of a 50 % slurry of ANTI-FLAG M2 Affinity Gel (Sigma–Aldrich) that had been pre-equilibrated with 1 × TEZ buffer (50 mM Tris-HCl [pH 7.5], 1 mM EDTA, 10 mM $ZnCl_2$, 5 mM β-ME, and protease inhibitors). Then, the beads were washed with 40 mL of 1 × TEZ plus 500 mM ammonium sulfate, followed by a second wash with 40 mL of 1 × TEZ plus 50 mM ammonium sulfate. After equilibration of the column with 1 × TEZ plus 100 mM ammonium sulfate, 3 ng of 3×Flag Peptide (Sigma-Aldrich), was added to the resin beads and incubated for 1 h at 4°C for competing the elution. The protein was then eluted with three column volumes of 1 × TEZ plus 100 mM ammonium sulfate, 10 % glycerol was added, and the resulting aliquot was snap-frozen in liquid nitrogen and temporarily stored at -80°C.

2.4. Chromosomal genetic complementation of the rbf mutant strain

To construct the *rbf* chromosomal complementation, as previously described (Zhu et al., 2019), the DNA fragment of the full-length Rbf ORF and the flank upstream and downstream regions were amplified by PCR, using NCTC8325 and MW2 genomic DNA as template. The PCR products were then digested with EcoRI and KpnI, and then ligated into the pBTS vector, generating the plasmid pBTS-up-*rbf*-down. This plasmid was transformed into *S. aureus* RN4220 by electroporation, then electroporated into the *rbf* mutant strains. The transformants with homologous recombination were selected on TSB agar containing 200 ng/μl Anhydrotetracycline (ATC), and further verified by PCR and sequencing.

2.5. Electrophoretic mobility shift assay

For electrophoretic mobility shift assay (EMSA), the 3′-biotin-labeled DNA fragments p*hla* and p*psmα* containing the promoter regions were amplified from the *S. aureus* NCTC8325 genomic DNA using the primers in Table 2. Then the biotin-labeled DNA fragment (Rodgers et al., 2000) was incubated at 25°C for 20 min with various amounts of Rbf (0–2 pmol) in 10 μl of incubation buffer (10 mM Tris-HCl, pH 8.0, 100 mM NaCl, 1 mM EDTA). After incubation, the mixtures were added

Table 2
Oligonucleotide primers used in this study.

Primer	Oligonucleotide (5'-3')[a]	Application
RT-*hu*-F	AAAAAGAAGCTGGTTCAGCAGTAG	RT-real-time PCR
RT-*hu*-R	TTTACGTGCAGCACGTTCAC	RT-real-time PCR
RT-*rbf*-F	CGATATGCGTATTATGGTGATT	RT-real-time PCR
RT-*rbf*-R	AAGTAAGTGGAATTGTGATGAC	RT-real-time PCR
RT-*hla*-F	AGCAGCAGATAACTTCCT	RT-real-time PCR
RT-*hla*-R	TGGTAGTCATCACGAACT	RT-real-time PCR
RT-*psmα*-F	GTATCATCGCTGGCATCA	RT-real-time PCR
RT- *psmα*-R	AAGACCTCCTTTGTTTGTTATG	RT-real-time PCR
RT-*sarX*-F	AACATTGCTTGGCTTCTAT	RT-real-time PCR
RT-*sarX*-R	AATCTAGCTCATCCATTGC	RT-real-time PCR
RT-*icaA*-F	GAATATGGCTGGACTCA	RT-real-time PCR
RT-*icaA*-R	ATGCGACAAGAACTACT	RT-real-time PCR
RT-*lukD*-F	TGTTGTTGACTATGCACCTA	RT-real-time PCR
RT-*lukD*-R	CCACCTGATAAGCCATTAGA	RT-real-time PCR
RT-*lukE*-F	GAGTTATGTCAGTGAAGTAGAC	RT-real-time PCR
RT-*lukE*-R	CTTGCTGAACCTGTTGGA	RT-real-time PCR
RT-*chp*-F	GGCAGGAATCAGTACACA	RT-real-time PCR
RT-*chp*-R	TGTTGTAGGAAGACCACTAT	RT-real-time PCR
rbf-up-F	GCGGAATTCGAGCTCGGTACCCAGGTGTACTTGCCTTTCT	*rbf* deletion
rbf-up-R	CAAACCAATCGCTACTCAAA	*rbf* deletion
rbf-down-F	TTTGAGTAGCGATTGGTTTGTGATAAAAATGGATTTAAAA	*rbf* deletion
rbf-down-R	CTTGCATGCCTGCAGGTCGACTCAAAATGTTGCACCCCCAA	*rbf* deletion
C-*rbf*- F	CCGGAATTCGAGCTCGGTACCCAGGTGTACTTGCCTTTCT	*rbf* chromosomal complementation
C-*rbf*- R	CTTGCATGCCTGCAGGTCGACTCAAAATGTTGCACCCCCAA	*rbf* chromosomal complementation
pLI*rbf*-F	CCGGAATTCAGGTGTACTTGCCTTTC	Overexpression *rbf*
pLI*rbf*-R	CGCGGATCCAGCCATTGTCTTTCTC	Overexpression *rbf*
E-*rbf*- F	CCGGAATTCAGGTGTACTTGCCTTTC	Rbf expression
E-*rbf*- R	GCGGGATCCTTACTTATCGTCGTCATCCTTGTAATCCTTATCGTCGTCATCCTTGTAATCTTTTTTTCCTATTTTAATTA	Rbf expression
p*hla*-F	CCGACGAAATTCCAAACATA	EMSA
p*hla*-R	TAGTGTTGTTGTTACTGAG	EMSA
p*hla*-R-biotin	TAGTGTTGTTGTTACTGAG	EMSA(3' biotin)
p*psmα*-F	TCTGTTCAATTCATCTTCATA	EMSA
p*psmα*-R	GCCAGCGATGATACCCATTAAG	EMSA
p*psmα*-R-biotin	GCCAGCGATGATACCCATTAAG	EMSA(3' biotin)
lacZ-hla-F	CCGGAATTCCCGACGAAATTCCAAACATA	*lacZ* report
lacZ-hla-R	CGCGGATCCGGCATTAGCGACAGGATT	*lacZ* report
lacZ-psmα-F	CCGGAATTCTCTGTTCAATTCATCTTCATA	*lacZ* report
lacZ-psmα-R	CGCGGATCCCCGCCAGCGATGATACCCATTAAG	*lacZ* report

with 2 μl of gel loading buffer and then electrophoresed in a 5% native polyacrylamide gel in 1× Tris–borate–EDTA buffer. The band shifts were detected and analyzed with the Chemiluminescent Nucleic Acid Detection Module Kit (Thermo Fisher), and images were obtained by ImageQuant LAS 4000 (GE, Healthcare, NJ). The unlabeled fragments of each promoter were added to the labeled fragment at a ratio of approximately 100:1 as a specific competitor. The unlabeled fragment of the *hu* ORF region (100-fold) was added as a nonspecific competitor.

2.6. Construction of LacZ reporter plasmids

For the reporter plasmid pOS*psmα*, the 308-bp fragment of the *psmα* native promoter and a region of the first 18 bp of the *psmα* coding sequence were amplified from *S. aureus* NCTC8325 genomic DNA with a pair primers lacZ-*psmα*-F and lacZ-*psmα*-R (Table 2). The fragment was digested with BamHI/EcoRI and cloned into the shuttle vector pOS1 to generate reporter plasmid pOS*psmα*. The same protocol was followed to construct the reporter plasmids pOS*hla* using primers lacZ-*hla*-F and lacZ-*hla*-R (Table 2). The constructed plasmids were first introduced into *S. aureus* strain RN4220 for modification and subsequently transformed into NCTC8325 and the *rbf* mutant strain.

2.7. Construction of the rbf mutant strain

To construct the *rbf* mutant strain from *S. aureus* strain MW2, the downstream and upstream regions of *rbf* were amplified from *S. aureus* MW2 genomic DNA using the *rbf*-up-F/*rbf*-up-R, *rbf*-down-F /*rbf*-down-R sets of primers (Table 2) and ligated by overlap PCR to form an up-down fragment. The product up-down fragment was digested with KpnI and SalI and cloned into the temperature-sensitive shuttle vector pBTs. The resulting plasmid pBTs*rbf* was first transformed into *S. aureus* RN4220 by electroporation for modification and then transformed into *S. aureus* MW2. The allelic replacement of *rbf* was selected using a previously described method (Zhu et al., 2019) and was further verified by PCR and sequencing.

2.8. Construction of overexpression plasmids

To construct the *rbf* overexpression plasmid, the fragment covering *rbf* and its promoter regions was amplified from strain MW2 and NCTC8325 genomic DNA with primers pLI*rbf*-F and pLI*rbf*-R (Table 2). The fragment was digested with EcoRI/ BamHI and cloned into the shuttle vector pLI50 (Lee et al., 1991) to obtain pLI*rbf*.

2.9. β-Galactosidase activity assay

For β-galactosidase activity assays, stationary-phase cultures of the WT strain and *rbf*mutant strain containing different LacZ reporter plasmids were diluted 1:100 into TSB with chloromycetin. Bacterial cells were collected at the early-exponential phase (OD_{600} = 1) and mid-exponential phase (OD_{600} = 2), then thoroughly lysed at 37℃ with 100 μl ABT LSA buffer (60 mM K_2HPO_4, 40 mM KH_2PO_4, 100 mM NaCl, 0.01 % Triton X-100, 50 μg/mL lysostaphin). 100 μl ABT buffer (60 mM K_2HPO_4, 40 mM KH_2PO_4, 100 mM NaCl, 0.01 % Triton X-100) and 100 μl 4 mg/mL ONPG (o-nitrophenyl-β-D-galactopyranoside) were added to initiate the reaction. The samples were incubated at 37℃ until a yellow color became apparent, and then 1 mL Na_2CO_3 was added to stop the reaction. The galactosidase activity was analyzed according to

the method described previously(Xue et al., 2009).

2.10. Total RNA extraction, cDNA generation, and real-time quantitative reverse transcription PCR

Overnight cultures of *S. aureus* were diluted 1:100 in TSB and then grown to the certain cell density (OD_{600} = 1, OD_{600} = 2 and OD_{600} = 5) until being collected. The collected cells were processed with 1 mL of RNAiso Plus (TaKaRa) in combination with 0.1-mm-diameter-silica beads in a FastPrep-24 automated system (MP biomedicals Solon, OH, USA), and the residual DNA was removed with RNase-free DNase I (TaKaRa). The concentration of total RNA was adjusted to 200 ng/μl. Reverse transcription was performed with the PrimeScript 1 st Strand cDNA synthesis kit (Takara) and quantitative reverse transcription-PCR (qRT-PCR) was performed with SYBR Premix Ex Taq (TaKaRa) using a StepOne real-time system (Applied Biosystems). The relative quantity of cDNA measured by real-time PCR was normalized to the average abundance of WT strain samples using *hu* (encoding histone-like DNA-binding protein) as the reference gene for its stability of expression (Valihrach and Demnerova, 2012).

2.11. Hemolytic activity assay

For hemolytic activity assay, bacterial culture supernatants (100 μl) collected by the mid-logarithmic growth phase (OD_{600} of 2.5) were mixed with 900 μl phosphate-buffered saline (PBS) buffer containing 3% sheep erythrocytes. After incubated at 37°C for proper time until the hemolytic effect can be observed (NCTC8325 strain for 30 min and MW2 strain for 90 min), the absorption of supernatant at 543 nm was measured after centrifugation (8000 rpm, 2 min). A mixture with 1000 μl ddH_2O containing 3% sheep erythrocytes was used as the positive control, and a mixture with 1000 μl PBS containing 3% sheep erythrocytes was used as the negative control. The percentage of hemolytic activity was calculated relative to the positive control, which was regarded as 100 % hemolytic activity.

2.12. Mouse subcutaneous abscess model

Outbred, immunocompetent female BALB/c mice between 6 and 7 weeks of age were used for the abscess model. The hair on the back was removed by an animal shaver. *S. aureus* strains were grown to mid-exponential phase, washed once with sterile PBS, and then resuspended in PBS at 5×10^7 colony-forming units(CFU)/50 μl. Mice were anesthetized with isoflurane and inoculated with 50 μl PBS containing 10^7 CFU of live *S. aureus* or PBS alone in the right flank by subcutaneous injection. Abscess areas, assessed as the maximal length times width of the developing ulcers, were measured daily. The skin lesions were excised and homogenized in water after 7 days. The number of CFU recovered from each individual lesion was counted by serial dilution and plated onto TSB agar plates. For histopathological analyses, the skin lesions were placed in 10 % formalin. Paraffin embedding and hematoxylin and eosin (H&E) staining were performed by Wuhan Servicebio Technology.

2.13. mRNA half-life assay

Overnight cultures of *S. aureus* were inoculated at 1:100 into TSB medium and grown for 4 h. Cultures were treated with rifampin (200 μg/mL) for 0, 5, 10, or 20 min. Cells then were collected after rifampin treatment and processed for RNA isolation, and then the hla and *psmα* mRNA levels were measured by qRT-PCR.

2.14. Butanol extraction of PSMs

PSM peptides in culture supernatants were isolated by the butanol extraction method as previously described (Joo and Otto, 2014; Zapf et al., 2019). To isolate the PSM peptides, the strains were grown in TSB and incubated at 37°C with shaking at 220 rpm for 8 h. Five milliliters supernatants were clarified by filtration, then combated with 2 mL 1-butanol. The solutions were incubated with vigorously shaking at 37°C for 2 h. After this incubation, upper (butanol) phases was collected after brief centrifugation and dried by vacuum centrifugation. To visualize PSM peptides, the extracts dissolved in water were separated on SDS-12 % polyacrylamide gels and stained with Coomassie brilliant blue.

2.15. PSM measurements

PSMs were measured by high-pressure liquid chromatography/electrospray ionization mass spectrometry (HPLC/ESI-MS) as previously described (Joo and Otto, 2014). The amount of PSM is expressed as the integral intensity of the main two peaks detected in the ion chromatogram of the respective peak in the total ion chromatogram.

2.16. Western blot analysis

To determine the protein expression level of Hla, the strains were grown in TSB medium at 37°C with shaking (220 rpm) 8 h. The production of Hla in the supernatants of the *S. aureus* cultures was determined by western blot analysis. To standardize the total protein concentration of the supernatants, the SDS-PAGE and the bicinchoninic acid (BCA) assay were performed. Then equivalent volumes (20 μl each) of supernatants were separated by 12 % SDS-PAGE and electrotransferred onto a polyvinylidene difluoride membrane (GE, Piscataway, NJ). The protein was detected with a rabbit anti-alpha-toxin antibody (Sigma) followed by horseradish peroxidase-conjugated sheep anti-rabbit antibodies (Pierce) and quantified with Image J software.

2.17. Ethics statement

The use and care of mice in the present study followed strictly the guidelines adopted by the Ministry of Health of the People's Republic of China in June 2004. The protocol was approved by the Institutional Animal Care and Use Committee of the University of Science and Technology of China (USTCACUC192001037).

2.18. Statistics

Statistical analysis was performed using Graph Pad Prism version 7.00. For the comparison of two groups, unpaired t tests were used; for three or more groups, 1-way or 2-way analysis of variance (ANOVA) was used, as appropriate. All error bars depict the standard errors of the means.

3. Results

3.1. Impact of Rbf on hemolytic activity

Previous studies have revealed that Rbf can increase biofilm formation by promoting the production of PIA (Cue et al., 2013, 2009). To explore its other regulatory function of virulence, we constructed the *rbf* mutant strains of NCTC8325 and MW2 (clinical MRSA strain) by allelic exchange and complemented the resulting mutants harboring an introduced *rbf* chromosomal copy for genetic complementation. Using the *rbf* mutant and the complemented strains of NCTC8325, we performed the hemolytic activity assay. By measuring the absorption of supernatants at 543 nm, the percentage of hemolytic activity was calculated relative to the positive control (100 % hemolytic activity). As shown in Fig. 1A, the percentage hemolytic activity of the *rbf* mutant strain increased 2.5-fold compared to that in the WT strain. And all the observed effects can be well restored by the complemented strain. To further verify this phenomenon, we performed the hemolytic activity assays in the clinical MW2 strains, and the result was consistent with the phenomenon in NCTC8325 strains (Fig. 1B). Meanwhile, no significant difference in growth was observed between the WT and *rbf*

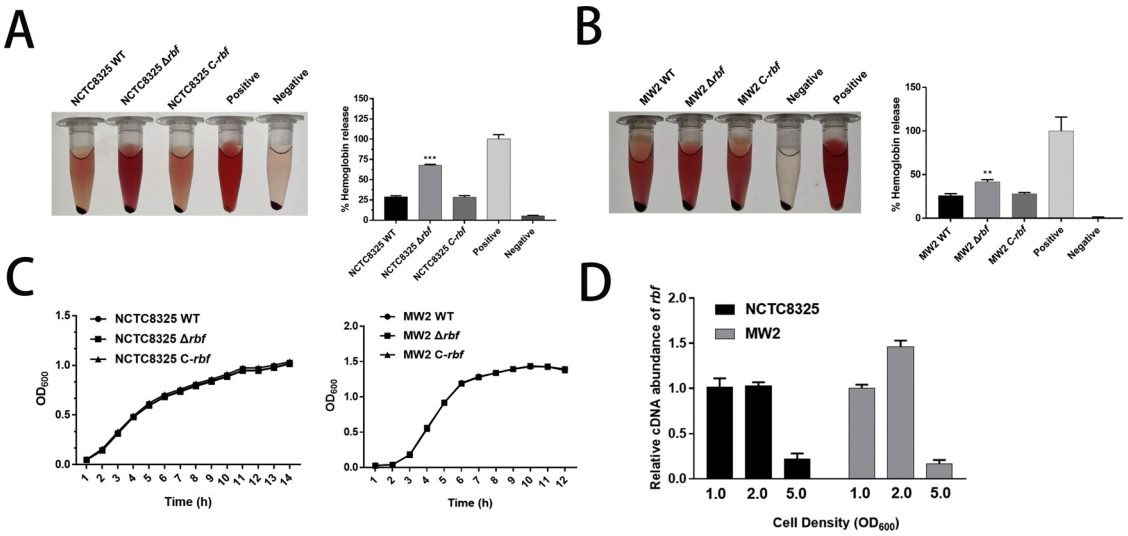

Fig. 1. Negative regulation of Rbf on hemolytic activity. (A) Hemolytic activity of the *rbf* mutant of strains NCTC8325 and MW2 (B). After incubated at 37℃ for proper time until the hemolytic effect can be observed (NCTC8325 strain for 30 min and MW2 strain for 90 min), the absorption of supernatant at 543 nm was measured after centrifugation (8000 rpm, 2 min). Relative hemolytic activity was calculated by the positive control (100 % hemolytic activity). ***, $P < 0.001$, **$P < 0.01$. (C) Growth of the WT, the *rbf* mutant, and the *rbf* chromosomal-complemented in *S. aureus* strains NCTC8325 and MW2. (D) Growth-dependent expression of *rbf* determined by qRT-PCR in S. *aureus* strains NCTC8325 and MW2.

mutant strains (Fig. 1C). To analyze the expression level of *rbf* at different growth phases, we detected the transcript level of *rbf* in early exponential (OD_{600} = 1), mid-exponential (OD_{600} = 2), and stationary phases (OD_{600} = 5). Our results showed that the transcript level of *rbf* is higher in early exponential and mid-exponential phases (Fig. 1D), indicating that its expression is growth phase dependent. Taken together, these data show that the *rbf* mutant strain exhibited increased hemolytic activity compared to that in WT strain.

3.2. Rbf inhibits the expression of virulence genes hla and psmα

To determine the regulatory impacts of virulence-related genes in the *rbf* mutant strain, we focus on several virulence genes and use qRT-PCR to examine their transcript levels. As shown in Fig. 2A, the transcript levels of *hla* and *psmα* in the *rbf* mutant strains increased about 4.3-fold and 4.8-fold, respectively, compared to that in the WT strain. The results indicated that *rbf* negatively regulates the expression of *hla* and *psmα*, encoding alpha-hemolysin (Song et al., 1996) and four PSMα peptides, respectively (Wang et al., 2007), which play a preeminent role in a variety of severe diseases in staphylococcal infections (Otto, 2014). Clinical methicillin-resistant *Staphylococcus aureus* strain MW2 was reported to produce PSM peptides abundantly (Wang et al., 2007). To further investigate whether Rbf can regulate the transcriptions of *hla* and *psmα* in clinical *S. aureus* strains, we performed qRT-PCR in the WT, *rbf* mutant, and complemented strains of MW2. The transcript levels of *hla* and *psmα*significant inceased in MW2 *rbf* mutant strain compared to MW2 WT strain in consistent with the observed in NCTC8325(Fig. 2B). Since mRNA stability can affect the expression of virulence factors in addition to the transcription (Roberts et al., 2006), we performed mRNA half-lives assays. Our results showed that the mRNA levels in the *rbf* mutant strain were attenuated at similar rates in the WT and *rbf* chromosomal genetic complemented strains (Fig. 2C). Moreover, to characterize the regulation of *hla* and *psmα* in the *rbf* mutant strain, we checked the transcript levels of *hla* and *psmα* at different growth phases. As shown in Fig. 2D, at different growth phases (OD_{600} = 1, OD_{600} = 2, OD_{600} = 5), the transcript levels of *hla* and *psmα* increased 3.9, 6.3, 4.1 fold and 3.7, 2.7, 2.8 fold compared to that in the WT strain. These results indicated that *rbf* can inhibit the transcript levels of *hla* and *psmα* in growth-dependent manner. To further investigate the regulatory roles of Rbf, we constructed the *hla* and *psmα* promoter-*lacZ* fusion reporter plasmids and detected the β-galactosidase activities in the WT and *rbf* mutant strains. As shown in Fig. 2E, the mean β-galactosidase activities of *hla* and *psmα* promoter exhibited 1.9-fold and 1.8-fold increase, respectively, in the *rbf* mutant strain compared to that in the WT strain at mid-exponential phase (OD_{600} = 2). ***$P < 0.001$. These results further indicated that Rbf is a negative regulator of *hla* and *psmα*. To investigate the direct linkage of *hla* and *psmα* expression to hemolytic activity, the mid-exponential phase strain was incubated with 3% sheep erythrocytes for 20 min. Cells were then collected, total RNA was extracted, and qRT-PCR was performed. The results showed that the transcript levels of *hla* and *psmα* increased 3.2-fold and 3.1-fold in the *rbf* mutant strain compared to that in WT strain in the hemolytic assay processes (***$P < 0.001$, **$P < 0.01$) (Fig. 2F). To further demonstrate that Rbf can inhibit the expression of *hla* on protein level, we performed western blot and densitometry-determined by Image J software. The *rbf* mutant strain displayed 2.8-fold higher protein level of Hla than that in WT strain. ***$P < 0.001$. These results demonstrated that Rbf can repress the expression of Hla (Fig. 2G). To analyze the protein level of PSMα peptides, butanol extraction was performed to isolate and purify the PSM peptides from the filtrated culture supernatants of *S. aureus*. The extracts were analyzed by 12 % SDS-PAGE, and the results showed that one band corresponding to PSMs (Fig. S3). And *rbf* mutant strain exhibited increased level of PSMs abundance compared to WT strain and complementary strain of NCTC8325 and the clinical strain MW2 (Fig. 2H). To further substantiate the protein level of PSMα peptides, the production of PSMs (PSMα and PSMβ peptides, δ-toxin) was determined by HPLC/MS. As shown in Fig. 2I, the production of PSMα peptides was significantly increased in NCTC8325 *rbf* mutant strain compared to the WT strain. Meanwhile, PSMβ peptides showed slightly increased production in the NCTC8325 mutant strain compared to the corresponding WT strain. Results obtained for PSMα3, PSMα4, and PSMβ1 are shown in Fig. 2I as examples for the PSMα and PSMβ peptides, which are encoded by the *psmα* and *psmβ* operons, respectively, and their respective products are linked in expression (Cheung et al., 2014). Differences in abundance of the δ-toxin were no significant in a comparison of the NCTC8325 WT strain and *rbf* mutant strain shown in Fig. 2I, and the level of PSMs increased mainly due to the increased level of PSMα in the *rbf* mutant strain compared to the WT strain. Together, these results demonstrate that Rbf plays a repressive role in the expression of virulence genes of *hla* and *psmα*.

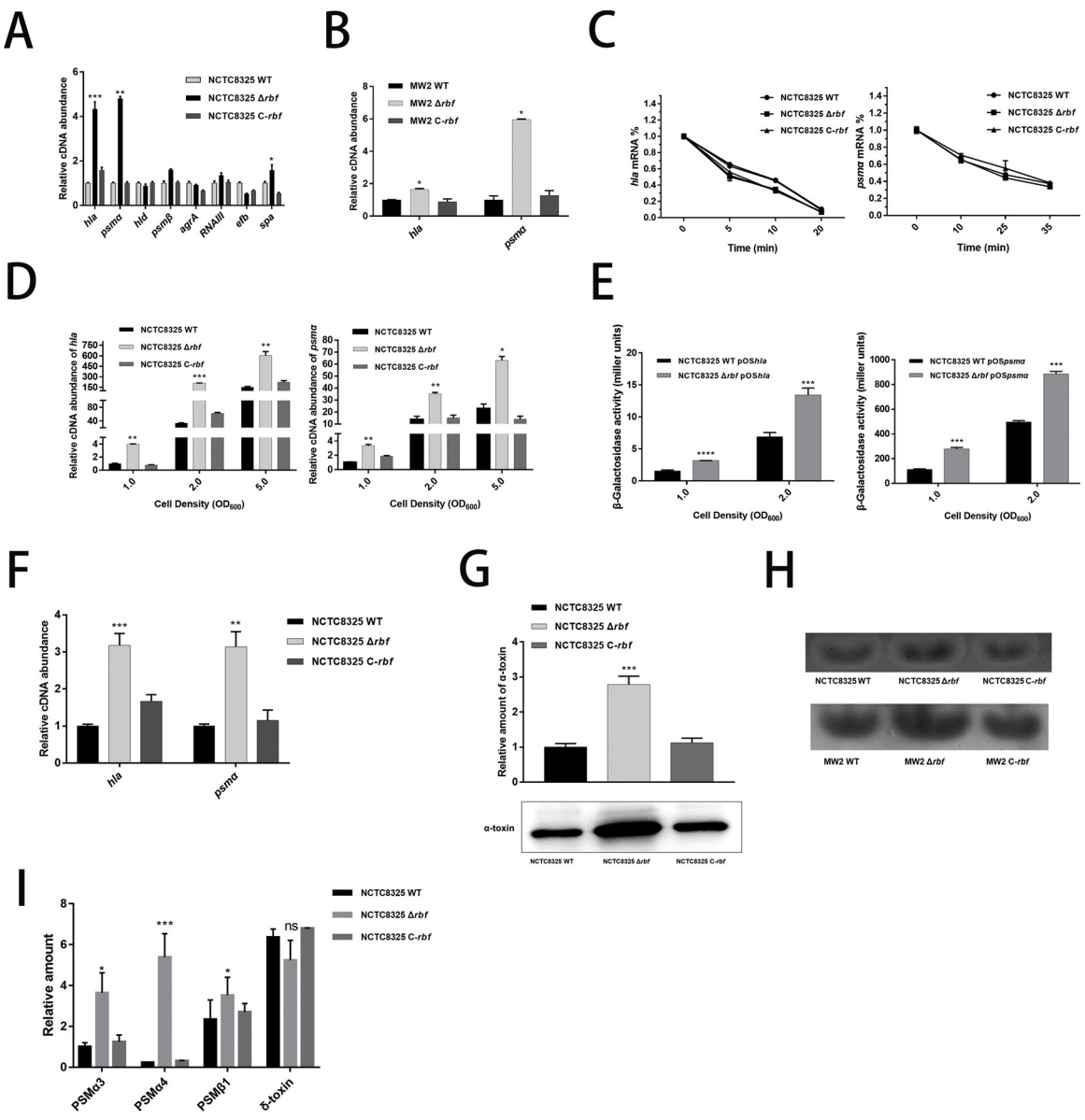

Fig. 2. Rbf inhibits the expression of virulence genes *hla* and *psmα* in *S.aureus*. (A) The transcript levels of virulence genes in the WT, *rbf* mutant, and *rbf* chromosomal-complemented strains of NCTC8325. (B) The transcript levels of *hla* and *psmα* in the WT,*rbf* mutant, and *rbf* chromosomal-complemented strains of MW2. (C) The mRNA half-life analysis of *hla* and *psmα* in the WT, *rbf* mutant, and *rbf* chromosomal-complemented strains. (D) Growth-dependent transcript level analysis of *hla* and *psmα* determined by qRT-PCR in the WT and *rbf* mutant strains of NCTC8325. (E) The β-Galactosidase activities driven by the *hla* and *psmα* promoters in the WT and *rbf* mutant strains of NCTC8325. Bacterial cells were collected at the indicated cell density points, and the substrate ONPG was used for the β-galactosidase activities. (F) Detection of *hla* and *psmα* mRNA levels in hemolytic activity assay. (G) Western blot analysis of alpha-toxin production in the supernatants of the WT, *rbf* mutant, and *rbf* chromosomal-complemented strains of NCTC8325 after grown in TSB medium for 8 h. (H) Production of PSM peptides was measured by Coomassie blue-stained SDS-PAGE of butanol extracts. A band with increased intensity was observed in *rbf* mutant compared to WT strains of NCTC8325 and MW2. (I) Production of PSM peptides and δ-toxin was measured by HPLC/MS in culture filtrates (8 h of growth). Abundance values are expressed as combined intensity of the two most abundant *m/z* peaks for every peptide. PSMα3 and PSMα4 is shown as an example for PSM peptides and PSMβ1 for PSMβ peptides. Error bars, replicates ± SEM. Comparisons were determined by the Student's *t* test, one-way ANOVA, and the F test to compare variances. *P < 0.05, **P < 0.01, ***P < 0.001, ****P < 0.0001, ns indicates no significant.

3.3. Overproduction of Rbf leads to decreased expression levels of hla and psmα

To further confirm that Rbf plays a critical role in the regulation of *hla*and*psmα*, we constructed the *rbf* overproduction strains with a plasmid harboring *rbf* gene and tested the effect of overexpression. The transcript level of *rbf* in the *rbf*-overexpression strain increased 9-fold compared with the WT strain with an empty plasmid pLI50 (Fig. S2). To investigate whether overproduction of Rbf can affect the hemolytic activity, the hemolytic assays were performed, and the results showed that overproduction of *rbf* in NCTC8325 strain could result in the deceased hemolytic activity (Fig. 3A). The consistent result was observed in clinical MW2 strain (Fig. 3B). Growth of the NCTC8325 *rbf*-overexpression strain was slightly slower compared to that in NCTC8325 WT strain. Similar growth results were observed in clinical MW2 strain (Fig. 3C). Furthermore, qRT-PCR results showed that the transcript levels of *hla*and*psmα* decreased obviously in the *rbf*-overexpression strain compared to that in the WT strains NCTC8325 and MW2 (Fig. 3D). To analyze the protein level of Hla in the *rbf*-overexpression strain, we performed the western blot assay. As shown in Fig. 3E, the relative

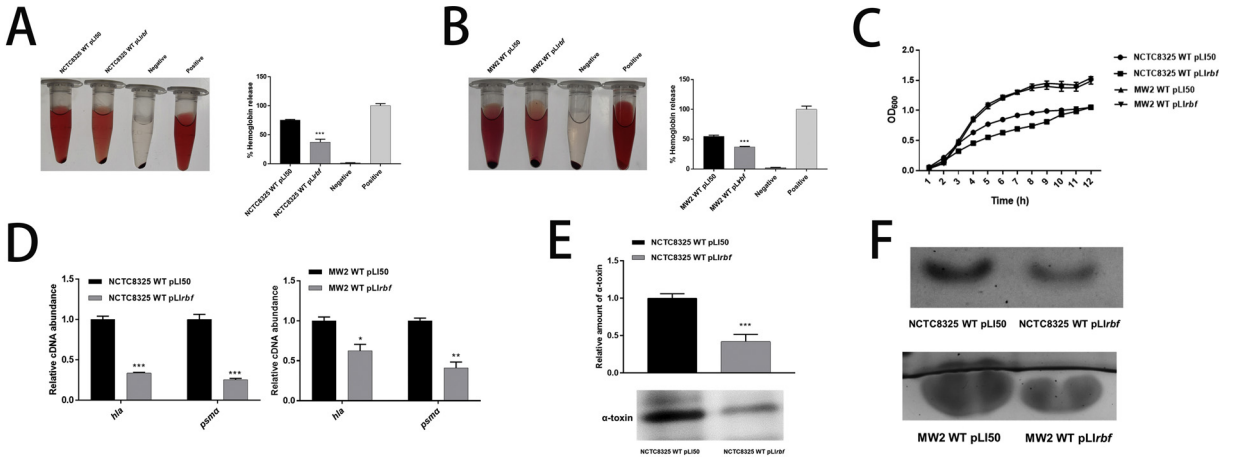

Fig. 3. Overproduction of *rbf* leads to decreased *hla* and *psmα*expression levels. (A) Hemolytic activity analysis of *rbf* overproduction and WT strains of NCTC8325 and MW2 (B). (C) Growth of the WT and *rbf* overproduction strains of NCTC8325 and MW2. (D) The transcript levels of *hla* and *psmα* in the WT and *rbf*-overexpression strains of NCTC8325 and MW2. (E) Western blot analysis of alpha-toxin production of the *rbf*-overexpression strain and WT strain. (F) PSM peptides levels are significantly decreased in the *rbf*-overexpression strains compared to the WT strains of NCTC8325 and MW2. Culture supernatants filtrates (8 h of growth) were butanol extracted and analyzed by 12 % SDS-PAGE. Statistical significance was determined by the Student's *t* test. *P < 0.05, **P < 0.01, ***P < 0.001.

amount of Hla decreased 2.4-fold in the *rbf*-overexpression strain compared to that in the WT strain. Meanwhile the protein level of PSMα peptides was determined by SDS-PAGE analysis of butanol extractions. Decreased PSM production was observed when *rbf* was overproduced in the WT strains of NCTC8325 and MW2 (Fig. 3F). Taken together, these results showed that overproduction of *rbf* in the WT strain of NCTC8325 and MW2 results in decreased *hla* and *psmα* expression levels. These data clearly demonstrate that Rbf can repress the expression of *hla* and *psmα*, and subsequently affect the virulence.

3.4. Rbf can specifically bind to the promoter regions of hla and psmα

As a member of the AraC/XylS family proteins, Rbf contains two predicted helix-turn-helix DNA-binding domains (Lim et al., 2004). To determine whether *hla* and *psmα* genes are under the direct control of Rbf, we expressed and purified FLAG-tagged Rbf. DNA fragments containing the potential promoter motifs were amplified and used for EMSA. The results showed that recombinant Rbf was able to bind to the *hla* promoter in a dose-dependent manner (Fig. 4A). Binding specificity was demonstrated by competing with a 100-fold excess of unlabeled *hla* promoter DNA and nonspecific competitors of the *hu* ORF region. The shifted band disappeared in the presence of a 100-fold concentration of unlabeled DNA of *hla* promoter, while the 100-fold nonspecific competitor *hu* did not have the competitive effect. EMSA was also performed using the potential promoter region of *psmα*, and similar band shift patterns were found (Fig. 4B). These results indicated that Rbf can specifically bind to the *hla* and *psmα* promoters.

3.5. Control of virulence in subcutaneous abscess infection of mice

To evaluate the impacts of the *rbf* mutant on virulence, we used murine models of skin infection to investigate the pathogenicity modulation of *rbf* to the skin and soft tissue infection (SSTI) in *S. aureus* NCTC8325. As measured by skin abscess sizes (Fig. 5A), the skin abscess sizes in the *rbf* mutant strain infected (~400 mm^2) was about 2-fold larger than the WT strain (~200 mm^2) in skin infection models, which was further demonstrated in images of skin dermonecrosis areas (Fig. 5B). Determination of the bacterial colonization of the lesion skin after 7 days of infection, the *rbf* mutant infected mice was 5.5 times higher than the WT-infected mice by the number of CFU, among which it is parallel with its increased lesion response. And the chromosomal genetic complementary strain can well restore these alterations (Fig. 5C). Histological examinations of the *rbf* mutant exhibited severer inflammation with destruction of skin structure and leukocyte infiltration (Fig. 5D).

4. Discussion

Rbf contained a consensus region signature of the AraC/XylS family, which was first identified as a transcriptional regulator and involved in the regulation of biofilm formation in response to glucose and salt (Lee et al., 1991; Lim et al., 2004). Further studies have demonstrated that Rbf and SarX represent a regulatory cascade that promotes PIA-dependent biofilm formation in *S. aureus* (Cue et al., 2013; Gallegos et al., 1997). These studies have provided a deep understanding of Rbf in biofilm formation. Biofilm formation is involved in chronic infections as

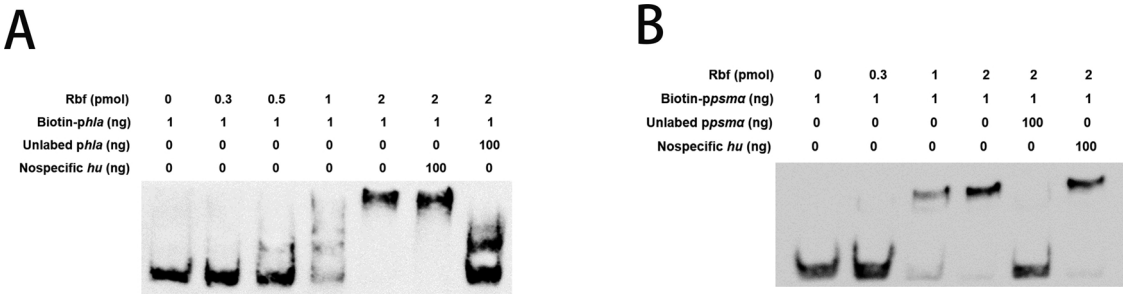

Fig. 4. Binding of Rbf to *hla* and *psmα* promoters. EMSA of purified Rbf with the biotin-labeled promoters p*hla* (A) and p*psmα* (B) was performed. The putative promoter regions of *hla* and *psmα* were amplified by the primers in Table 1, and incubated with increasing concentrations of Rbf. The unlabeled probes were added as specific competitors, and the unlabeled fragment of the *hu* ORF region was used as a non-specific competitor.

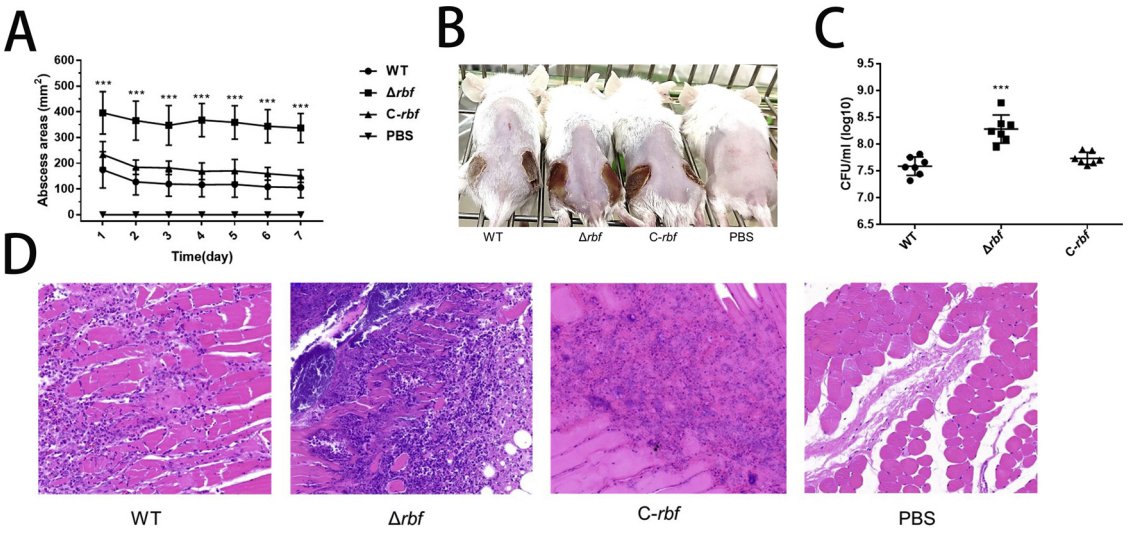

Fig. 5. The *rbf* mutant strain exhibited enhanced virulence in the mouse subcutaneous abscess infection. (A) Outbred, immunocompetent female BALB/c were injected subcutaneously with 5×10^7 live cells. Abscess or dermonecrosis areas were measured daily. ***, $P < 0.001$. (B) Representative example of the abscess and dermonecrosis area on Day 7 post-injection. (C) The number of CFU recovered at 7 days after infection was determined. ***, $P < 0.001$. (D) Representative H&E stained mouse abscessed areas histopathology images.

a long term evasion strategy, while toxin production as a virulence trait may cause acute infections (Otto, 2008, 2014). However, the detail regulatory mechanisms mediated by Rbf in virulence control still remain unclear.

In this study, we were interested in the virulence control by Rbf. We first performed hemolytic activity assays in the WT and *rbf* mutant strains and observed the extremely increased relative hemolytic activity in the *rbf* mutant strain. We investigated the transcript levels of genes encoding important toxins regulated by Rbf. Our data indicated that the transcript levels of *hla* and *psmα,* encoding alpha-toxin and PSMα, respectively, were significantly increased in the *rbf* mutant strain compared with the WT strain. Alpha-toxin and PSMα, as the important membrane-damaging toxins of *S. aureus*, can cause pore formation in the membrane. This pore formation can lead to the efflux of vital molecules and metabolites, and therefore is cytolytic and causes infection diseases (Otto, 2014). Results of β-galactosidase activity assay and EMSA revealed that Rbf can directly bind to the *hla* and *psmα* promoter regions to repress their expression in *S. aureus*. Furthermore, the increased production levels of alpha-toxin and PSMα explain well the difference in hemolytic capacity observed in the *rbf*mutant strains, as these are the most important hemolytic toxins of *S. aureus.* Meanwhile, the decreased expression levels of *hla* and *psmα* further confirmed the toxins control by Rbf in the *rbf*-overexpressed strain compared with the WT strains NCTC8325 and MW2.

Mouse subcutaneous abscess model can be used to investigate a number of virulence factors related to the pathogenesis of skin and soft tissue infections (Malachowa et al., 2013). In the model of mouse subcutaneous abscess, the *rbf* mutant strain exhibited significantly increased pathogenicity than that in the WT strain. In this study, alpha-toxin and PSMα, as the most important hemolytic virulence factors in *S. aureus,* showed significantly increased expression levels in the *rbf* mutant strain compared to that in the WT strain. In addition, to get comprehensive understanding of Rbf regulon, we performed qRT-PCR of infection-related virulence genes influenced by Rbf. As shown in Fig. S1, the result of qRT-PCR showed that the transcript levels of *lukED* and *chp* were increased in the NCTC8325 *rbf* mutant strain compared to that in WT strain. Leukotoxin ED (LukED), as a pore-forming toxin, was reported that targets the chemokine receptor CCR5, CXCR1, and CXCR2 to kill T lymphocytes, dendritic cells, and macrophages (Alonzo III et al., 2013; Reyes-Robles et al., 2013). Chemotaxis inhibitory protein of *S. aureus* (CHIPS) was reported that can reduce the neutrophil towards C5a and regarded an immune escape mechanism in *S. aureus* (de Haas, 2004). These researches suggest that LukED and CHIPS can be involved in staphylococcal infections and deserve further investigation in the Rbf regulon.

AraC-type transcriptional regulators known as Rbf can bind to DNA promoter regions, then elicit a negative or positive effect on the genes expression (Li et al., 2015; Yang et al., 2011). Here, the regulatory effect of Rbf on the expression of the *hla* and *psmα* is opposite to that of Rbf on the *sarX* promoter (Fig. 6), thus causing different infections, reflecting the diverse regulatory roles that Rbf can play as a global transcriptional factor.

Alpha-toxin and PSMα are categorized as membrane-damaging toxins, which are typical virulence factors of *S. aureus*. These virulence factors can attach to the cytoplasmic membrane in receptor-mediated or non-receptor mediated manners and lead to membrane distintegration, thus causing acute infections (Berube and Bubeck Wardenburg, 2013; Inoshima et al., 2011; Lugowski et al., 2018). Meanwhile, biofilm formation provides a protecting environment enabling the bacteria cells to proliferate by limiting antibiotic access and shielding the bacterial pathogen from host immune defense, which often causes chronic infections (Otto, 2010; Trotonda et al., 2008). The regulatory mechanisms that Rbf switches gene expression to generate those categorically different modes of infections may be interpreted as a response to the environmental changes that *S. aureus* encounter when breaching the host barrier, shielding host defense and coming in contact with a generally more hostile environment. These interpretations are considering the especially important role of AraC-like regulators such as Rbf, which can sense the environmental conditions by responding to chemical signals, then adjust the expression patterns of virulence genes (Gallegos et al., 1997; Yang et al., 2011).

In conclusion, we have revealed that Rbf can negatively regulate the hemolysis activity and directly repress the expression of *hla* and *psmα.* Furthermore, the *rbf* mutant strain exhibited significantly increased pathogenicity compared to the WT strain in the model of mouse subcutaneous abscess accordingly. Our findings provide a novel insight into the virulence regulation and acute infections mediated by Rbf in *S. aureus.*

Funding

This study was supported by the National Natural Science

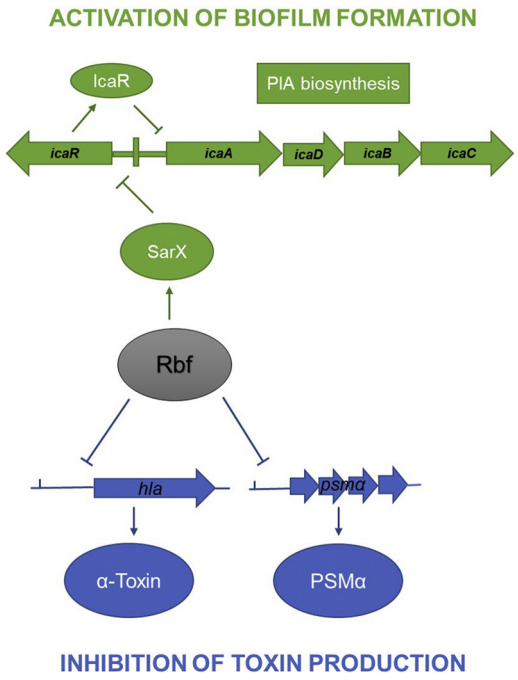

Fig. 6. Working model of Rbf regulatory mechanisms on virulence control in *S. aureus*. Bottom (blue): Rbf negatively regulates the production of α-toxin and PSMα. Rbf can directly bind to the promoter regions of *hla* and *psmα* to repress their expression. Top (green): Rbf positively regulates factors involved in biofilm formation, Rbf and SarX represent a regulatory cascade to inhibit IcaR, a negative regulator of *icaADBC*, and promote biofilm formation. Bars represent repression, whereas arrows represent activation. Previous studies are in green and our findings are in blue.

Foundation of China (31870126), and the Strategic Priority Research Program of the Chinese Academy of Sciences (XDB29020000).

Declaration of Competing Interest

No potential conflict of interest was reported by the authors.

Acknowledgments

We thank Zeyu Jin and Shuwan Qiu for technical assistance. We thank the Network on Antimicrobial Resistance in *Staphylococcus aureus* (NARSA) for providing the bacterial strains.

Appendix A. Supplementary data

Supplementary material related to this article can be found, in the online version, at doi:https://doi.org/10.1016/j.ijmm.2020.151436.

References

Alonzo III, F., Kozhaya, L., Rawlings, S.A., Reyes-Robles, T., DuMont, A.L., Myszka, D.G., Landau, N.R., Unutmaz, D., Torres, V.J., 2013. CCR5 is a receptor for *Staphylococcus aureus* leukotoxin ED. Nature 493, 51–55.
Archer, G.L., Climo, M.W., 2001. *Staphylococcus aureus* bacteremia–consider the source. N. Engl. J. Med. 344, 55–56.
Arvidson, S., Tegmark, K., 2001. Regulation of virulence determinants in *Staphylococcus aureus*. Int. J. Med. Microbiol. 291, 159–170.
Berube, B.J., Bubeck Wardenburg, J., 2013. *Staphylococcus aureus* alpha-toxin: nearly a century of intrigue. Toxins 5, 1140–1166.
Bronesky, D., Wu, Z., Marzi, S., Walter, P., Geissmann, T., Moreau, K., Vandenesch, F., Caldelari, I., Romby, P., 2016. *Staphylococcus aureus* RNAIII and its regulon link quorum sensing, stress responses, metabolic adaptation, and regulation of virulence gene expression. Annu. Rev. Microbiol. 70, 299–316.
Bunikowski, R., Mielke, M.E., Skarabis, H., Worm, M., Anagnostopoulos, I., Kolde, G., Wahn, U., Renz, H., 2000. Evidence for a disease-promoting effect of *Staphylococcus aureus*-derived exotoxins in atopic dermatitis. J. Allergy Clin. Immunol. 105, 814–819.
Cai, G., Imasaki, T., Takagi, Y., Asturias, F.J., 2009. Mediator structural conservation and implications for the regulation mechanism. Structure 17, 559–567.
Cheng, H.R., Jiang, N., 2006. Extremely rapid extraction of DNA from bacteria and yeasts. Biotechnol. Lett. 28, 55–59.
Cheung, A.L., Bayer, A.S., Zhang, G., Gresham, H., Xiong, Y.Q., 2004. Regulation of virulence determinants in vitro and in vivo in *Staphylococcus aureus*. FEMS Immunol. Med. Microbiol. 40, 1–9.
Cheung, A.L., Nishina, K.A., Trotonda, M.P., Tamber, S., 2008. The SarA protein family of *Staphylococcus aureus*. Int. J. Biochem. Cell Biol. 40, 355–361.
Cheung, G.Y.C., Hwang-Soo, J., Chatterjee, S.S., Michael, O., 2014. Phenol-soluble modulins – critical determinants of *staphylococcal* virulence. FEMS Microbiol. Rev. 38, 698–719.
Cue, D., Lei, M.G., Luong, T.T., Kuechenmeister, L., Dunman, P.M., O'Donnell, S., Rowe, S., O'Gara, J.P., Lee, C.Y., 2009. Rbf promotes biofilm formation by *Staphylococcus aureus* via repression of icaR, a negative regulator of icaADBC. J. Bacteriol. 191, 6363–6373.
Cue, D., Lei, M.G., Lee, C.Y., 2013. Activation of sarX by Rbf is required for biofilm formation and icaADBC expression in *Staphylococcus aureus*. J. Bacteriol. 195, 1515–1524.
de Haas, C.J.C., 2004. Chemotaxis inhibitory protein of *Staphylococcus aureus*, a bacterial antiinflammatory agent. J. Exp. Med. 199, 687–695.
Dinges, M.M., Orwin, P.M., Schlievert, P.M., 2000. Exotoxins of *Staphylococcus aureus*. Clin. Microbiol. Rev. 13, 16–34 table of contents.
Einhauer, A., Jungbauer, A., 2001. The FLAG peptide, a versatile fusion tag for the purification of recombinant proteins. J. Biochem. Biophys. Methods 49, 455–465.
Foster, T.J., 2005. Immune evasion by *staphylococci*. Nat. Rev. Microbiol. 3, 948–958.
Gallegos, M.T., Schleif, R., Bairoch, A., Hofmann, K., Ramos, J.L., 1997. Arac/XylS family of transcriptional regulators. Microbiol. Mol. Biol. Rev. 61, 393–410.
Hu, J., Zhang, X., Liu, X., Chen, C., Sun, B., 2015. Mechanism of reduced vancomycin susceptibility conferred by walK mutation in community-acquired methicillin-resistant *Staphylococcus aureus* strain MW2. Antimicrob. Agents Chemother. 59, 1352–1355.
Inoshima, I., Inoshima, N., Wilke, G.A., Powers, M.E., Frank, K.M., Wang, Y., Bubeck Wardenburg, J., 2011. A *Staphylococcus aureus* pore-forming toxin subverts the activity of ADAM10 to cause lethal infection in mice. Nat. Med. 17, 1310–1314.
Joo, H.S., Otto, M., 2014. The isolation and analysis of phenol-soluble modulins of *Staphylococcus epidermidis*. Methods Mol. Biol. 1106, 93–100.
Kraemer, G.R., Iandolo, J.J., 1990. High-frequency transformation of *Staphylococcus aureus* by electroporation. Curr. Microbiol. 21, 373–376.
Lee, C.Y., Buranen, S.L., Ye, Z.H., 1991. Construction of single-copy integration vectors for *Staphylococcus aureus*. Gene 103, 101–105.
Li, T., He, L., Song, Y., Villaruz, A.E., Joo, H.S., Liu, Q., Zhu, Y., Wang, Y., Qin, J., Otto, M., Li, M., 2015. AraC-type regulator rsp adapts *Staphylococcus aureus* gene expression to acute infection. Infect. Immun. 84, 723–734.
Lim, Y., Jana, M., Luong, T.T., Lee, C.Y., 2004. Control of glucose- and NaCl-induced biofilm formation by rbf in *Staphylococcus aureus*. J. Bacteriol. 186, 722–729.
Liu, Y., Mu, C., Ying, X., Li, W., Wu, N., Dong, J., Gao, Y., Shao, N., Fan, M., Yang, G., 2011. RNAIII activates map expression by forming an RNA-RNA complex in *Staphylococcus aureus*. FEBS Lett. 585, 899–905.
Lowy, F.D., 1998. *Staphylococcus aureus* infections. N. Engl. J. Med. 339, 520–532.
Lugowski, A., Nicholson, B., Rissland, O.S., 2018. Determining mRNA half-lives on a transcriptome-wide scale. Methods 137, 90–98.
Ma, R., Qiu, S., Jiang, Q., Sun, H., Xue, T., Cai, G., Sun, B., 2017. AI-2 quorum sensing negatively regulates rbf expression and biofilm formation in *Staphylococcus aureus*. Int. J. Med. Microbiol. 307, 257–267.
Malachowa, N., Kobayashi, S.D., Braughton, K.R., DeLeo, F.R., 2013. Mouse model of Staphylococcus aureus skin infection. Methods Mol. Biol. 1031, 109–116.
Nakagawa, S., Matsumoto, M., Katayama, Y., Oguma, R., Wakabayashi, S., Nygaard, T., Saijo, S., Inohara, N., Otto, M., Matsue, H., 2017. Staphylococcus aureus virulent PSMα peptides induce keratinocyte alarmin release to orchestrate IL-17-dependent skin inflammation. Cell Host Microbe 22, 667-677.e665.
Oliveira, D., Borges, A., Simoes, M., 2018. Staphylococcus aureus Toxins and Their Molecular Activity in Infectious Diseases. Toxins 10.
Otto, M., 2008. Staphylococcal Biofilms, Bacterial Biofilms. Springer, pp. 207–228.
Otto, M., 2010. *Staphylococcus* colonization of the skin and antimicrobial peptides. Expert Rev. Dermatol. 5, 183–195.
Otto, M., 2014. *Staphylococcus aureus* toxins. Curr. Opin. Microbiol. 17, 32–37.
Reyes-Robles, T., Alonzo 3rd, F., Kozhaya, L., Lacy, D.B., Unutmaz, D., Torres, V.J., 2013. *Staphylococcus aureus* leukotoxin ED targets the chemokine receptors CXCR1 and CXCR2 to kill leukocytes and promote infection. Cell Host Microbe 14, 453–459.
Roberts, C., Anderson, K.L., Murphy, E., Projan, S.J., Mounts, W., Hurlburt, B., Smeltzer, M., Overbeek, R., Disz, T., Dunman, P.M., 2006. Characterizing the effect of the *Staphylococcus aureus* virulence factor regulator, SarA, on log-phase mRNA half-lives. J. Bacteriol. 188, 2593–2603.
Rodgers, J.T., Patel, P., Hennes, J.L., Bolognia, S.L., Mascotti, D.P., 2000. Use of biotin-labeled nucleic acids for protein purification and agarose-based chemiluminescent electromobility shift assays. Anal. Biochem. 277, 254–259.
Rupp, M.E., Ulphani, J.S., Fey, P.D., Bartscht, K., Mack, D., 1999a. Characterization of the importance of polysaccharide intercellular adhesin/hemagglutinin of *Staphylococcus epidermidis* in the pathogenesis of biomaterial-based infection in a mouse foreign body infection model. Infect. Immun. 67, 2627–2632.
Rupp, M.E., Ulphani, J.S., Fey, P.D., Mack, D., 1999b. Characterization of *Staphylococcus epidermidis* polysaccharide intercellular adhesin/hemagglutinin in the pathogenesis of intravascular catheter-associated infection in a rat model. Infect. Immun. 67, 2656–2659.

Song, L., Hobaugh, M.R., Shustak, C., Cheley, S., Bayley, H., Gouaux, J.E., 1996. Structure of *staphylococcal* alpha-hemolysin, a heptameric transmembrane pore. Science 274, 1859–1866.
Takagi, Y., Chadick, J.Z., Davis, J.A., Asturias, F.J., 2005. Preponderance of free mediator in the yeast Saccharomyces cerevisiae. J. Biol. Chem. 280, 31200–31207.
Trotonda, M.P., Tamber, S., Memmi, G., Cheung, A.L., 2008. MgrA represses biofilm formation in *Staphylococcus aureus*. Infect. Immun. 76, 5645–5654.
Valihrach, L., Demnerova, K., 2012. Impact of normalization method on experimental outcome using RT-qPCR in *Staphylococcus aureus*. J. Microbiol. Methods 90, 214–216.
Wang, R., Braughton, K.R., Kretschmer, D., Bach, T.H., Queck, S.Y., Li, M., Kennedy, A.D., Dorward, D.W., Klebanoff, S.J., Peschel, A., DeLeo, F.R., Otto, M., 2007. Identification of novel cytolytic peptides as key virulence determinants for community-associated MRSA. Nat. Med. 13, 1510–1514.
Xue, T., Zhao, L., Sun, H., Zhou, X., Sun, B., 2009. LsrR-binding site recognition and regulatory characteristics in *Escherichia coli* AI-2 quorum sensing. Cell Res. 19, 1258–1268.
Yang, J., Tauschek, M., Robins-Browne, R.M., 2011. Control of bacterial virulence by AraC-like regulators that respond to chemical signals. Trends Microbiol. 19, 128–135.
Zapf, R.L., Wiemels, R.E., Keogh, R.A., Holzschu, D.L., Howell, K.M., Trzeciak, E., Caillet, A.R., King, K.A., Selhorst, S.A., Naldrett, M.J., Bose, J.L., Carroll, R.K., 2019. The small RNA Teg41 regulates expression of the alpha phenol-soluble modulins and is required for virulence in *Staphylococcus aureus*. Mbio 10, e02484–18.
Zhu, Q., Wen, W., Wang, W., Sun, B., 2019. Transcriptional regulation of virulence factors Spa and ClfB by the SpoVG-Rot cascade in *Staphylococcus aureus*. Int. J. Med. Microbiol. 309, 39–53.